J Nanopart Res (2016) 18:4
DOI 10.1007/s11051-015-3315-8

RESEARCH PAPER

Hydrothermal growth of TiO_2-CaP nano-films on a Ti–Nb-based alloy in concentrated calcium phosphate solutions

Hongwei Li · Tao Fu · Wen Li · Zafer Alajmi · Jiamao Sun

Received: 29 August 2015 / Accepted: 23 December 2015 / Published online: 6 January 2016

Abstract The Ti–Nb-based TLM alloy (Ti–25Nb–3Zr–2Sn–3Mo) was subjected to hydrothermal treatment in the concentrated $Ca_3(PO_4)_2$, $CaHPO_4$, and $Ca(H_2PO_4)_2$ solutions for the purpose of calcification. The treated samples are covered by films consisting of Ca-rich nano-crystallites (100–500 nm) and small nano-grains. XPS and XRD analyses reveal the formation of hydroxyapatite, TiO_2, and Nb_2O_5 at the sample surface. The sample hydrothermally treated in $CaHPO_4$ solution exhibits bioactivity by inducing the formation of apatite layer after soaking test in the simulated body fluid for 15 days. The work would provide a good bioactive surface modification method for Ti–Nb alloy implants with complex shapes and even pores.

Keywords Titanium · Hydrothermal · Calcium phosphate · TiO_2 · Bioactivity · Corrosion · Surface science

H. Li (✉) · W. Li
School of Materials Science and Engineering, Chang'an University, Xi'an 710064, China
e-mail: lihw74@foxmail.com

T. Fu (✉) · Z. Alajmi · J. Sun
Key Laboratory of Biomedical Information Engineering of Ministry of Education, School of Life Science and Technology, Xi'an Jiaotong University, Xi'an 710049, China
e-mail: taofu@mail.xjtu.edu.cn

Introduction

As a material for hard tissue implants, titanium has good corrosion resistance and excellent biocompatibility, but its elastic modulus (~110 GPa) is much higher than that of bone (1–30 GPa). In order to avoid the mismatch of elastic modulus and 'stress shielding,' low-modulus titanium alloys are thus developed, which are mainly Ti–Nb-based β or near β titanium alloys (Fu et al. 2011a; Zhou et al. 2009; Zheng et al. 2007). For example, the Ti–Nb-based TLM alloy (Yu and Zhou 2006) has an elastic modulus of ~60 GPa. The elastic modulus of titanium can be further reduced by porous structure (tens or hundreds of micrometers in size, Ryan et al. 2006) to favor bone growth and fit elastic modulus of cancellous bone, and the bioactive surface modification of porous titanium becomes an interesting topic in recent years.

Among the bioactive surface modification methods for biomedical titanium, the alkali-heat method is well known to induce apatite layer formation from the simulated body fluid (SBF). However, the alkali treatment decreased the strength of porous titanium (Lin et al. 2009). Note that the Ti–Nb-based alloys are less corrosion resistant to alkali solutions than pure titanium (Xiong et al. 2008; Zheng et al. 2007). This method and sol–gel coating method (Qu et al. 2011) involve high-temperature (e.g., 600 °C) treatments, which alters microstructure and mechanical properties of special titanium alloys, e.g., Ti–Nb alloy (Yamaguchi et al. 2012) and NiTi alloy (Fu et al. 2011b).

Electrochemical deposition is a low-temperature method to prepare calcium phosphate coatings on metallic substrate, but it has difficulty to produce uniform coating layer on the inner pore surface of porous titanium (Zhang et al. 2005).

Hydrothermal treatment is a low-temperature and easily operated method for surface modification of titanium (Hamada et al. 2002; Nakagawa et al. 2005; Fu et al. 2015), in which only small quantities of solute and solvent are consumed, and the modification layer is in nanometer thickness. The high-pressure environment greatly accelerates diffusion of the reactants. Thus, hydrothermal treatment is an ideal method for surface modification of titanium implants with complex shapes and even pores.

Calcium hydroxide and neutral $CaCl_2$ and $MgCl_2$ solutions were used to hydrothermally grow titania films containing Ca or Mg on titanium and Ti–Nb alloy (Shi et al. 2012; Nakagawa et al. 2005; Chen et al. 2009; Zheng et al. 2009), and the formed calcium compound layer was beneficial for bioactivity of the materials and osteoblast cell growth on them. The shortcomings of these methods are that the solutions have corrosive effect on titanium during hydrothermal treatments, and the obtained films do not contain phosphate.

In this work, hydrothermal treatment was carried out in the concentrated calcium phosphate solutions for calcification of TLM alloy. The surface structure, chemical composition, in vitro bioactivity, and corrosion resistance of the treated TLM alloy were investigated.

Materials and method

The TLM alloy sheet with a thickness of 0.6 mm supplied by Northwest Institute for Nonferrous Metal Research, China was sparkle cut into small pieces (size 10×10 mm^2). The plates were polished, ultrasonically cleaned in acetone, ethanol, and deionized water in sequence, and dried in air. The polished samples were hydrothermally treated in the $Ca_3(PO_4)_2$, $CaHPO_4{\cdot}2H_2O$, and $Ca(H_2PO_4)_2$ solutions with the concentration of 3.3, 10.0, and 10.0 mM, respectively. The molar concentrations of the saturated calcium phosphate solutions were quite different (Table 1). The filling ratio of solutions in the Teflon-lined autoclave was ~80 %. The sample stood vertically in the autoclave with the help of a titanium clamp. The autoclave was sealed and heated at 200 °C for 16 h. After the treatment, the samples were taken out, rinsed with deionized water for several times, and dried. The sample treated in water was also prepared as the control.

Surface morphology and elemental composition of the samples were analyzed with a scanning electron microscope (SEM, FEI Quanta 600F) equipped with the energy dispersive analysis of X-ray (EDX), and crystallography was examined by X-ray diffraction (XRD, CuK_α, X'Pert PRO). Elemental composition and chemical bonding state of the samples were examined by X-ray photoelectron spectroscopy (XPS, AlK_α, K-Alpha, VG). The hydrothermally treated TLM samples were soaked in the simulated body fluid (SBF, Kim et al. 1997, 45 ml, renewed every 3 days) at 37 °C for the in vitro bioactivity test. Corrosion resistance of the samples was evaluated by potentiodynamic polarization tests in 0.9 % NaCl solution on an electrochemical workstation (CS150, Corrtest®) at ambient conditions. A platinum electrode was used as counter electrode, and the saturated calomel electrode (SCE) was reference electrode.

Results and discussion

Surface morphology and elemental analyses

Surface morphologies of the hydrothermally treated TLM alloy samples are shown in Fig. 1. The sample treated in water (sample S0) is covered by a dense film consisting of fine nano-particles (size 80–100 nm).

Table 1 Solubility and corresponding concentration of calcium phosphates at 20 °C

Calcium phosphate	Solubility (g/100 mL)	Concentration (mM)
$Ca_3(PO_4)_2$	2.0×10^{-3}	0.064
$CaHPO_4$	4.3×10^{-3}	0.316
$Ca(H_2PO_4)_2$	1.8	76.90

The hydrothermally prepared TiO_2 nano-grains on Ti substrate are formed through a dissolution–precipitation mechanism (Shi et al. 2012). The scratches are still apparent, indicating small thickness of the TiO_2 film. For the sample treated in the $Ca_3(PO_4)_2$ solution (sample S1), small particles (20–30 nm) and big spheres (100–500 nm) are observed at the substrate surface. The samples treated in the $CaHPO_4$ and $Ca(H_2PO_4)_2$ solutions (samples S2 and S3) have similar morphologies, with kernel-like particles (400–500 nm) and small nano-leaves at the surface. EDX analysis reveals that the big particles have much higher Ca/Ti ratio than the nano-leaves (Fig. 2), which possibly indicates that the former are calcium phosphate crystallites and the latter are mainly TiO_2 grains. Since sample S2 has the moderate ratio of concentration to solubility (Table 1) and the largest quantity of calcium phosphate crystallites, it is thus subjected to further characterization and tests.

Chemical composition of sample S2 surface layer was examined by XPS analysis, with the Ti 2*p*, Nb 3*d*, Ca 2*p*, P 2*p*, and O 1*s* spectra shown in Fig. 3. Titanium at the sample surface presents mainly in the form of TiO_2, having the binding energies of 464.4 eV (Ti $2p_{1/2}$) and 458.7 eV (Ti $2p_{3/2}$). In Nb 3*d* spectrum,

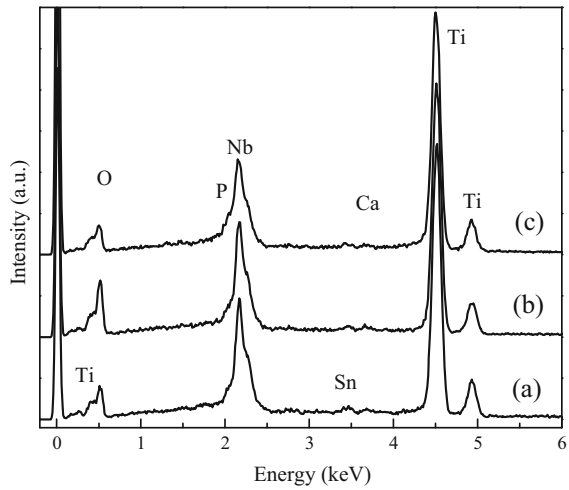

Fig. 2 EDX spectra of the TLM sample S2 taken at: **a** a nano-leaf, **b** a big particle, **c** the plan-view area in Fig. 1c. The atomic Ca/Ti ratio is 0.09, 0.51 and 0.38 %, respectively

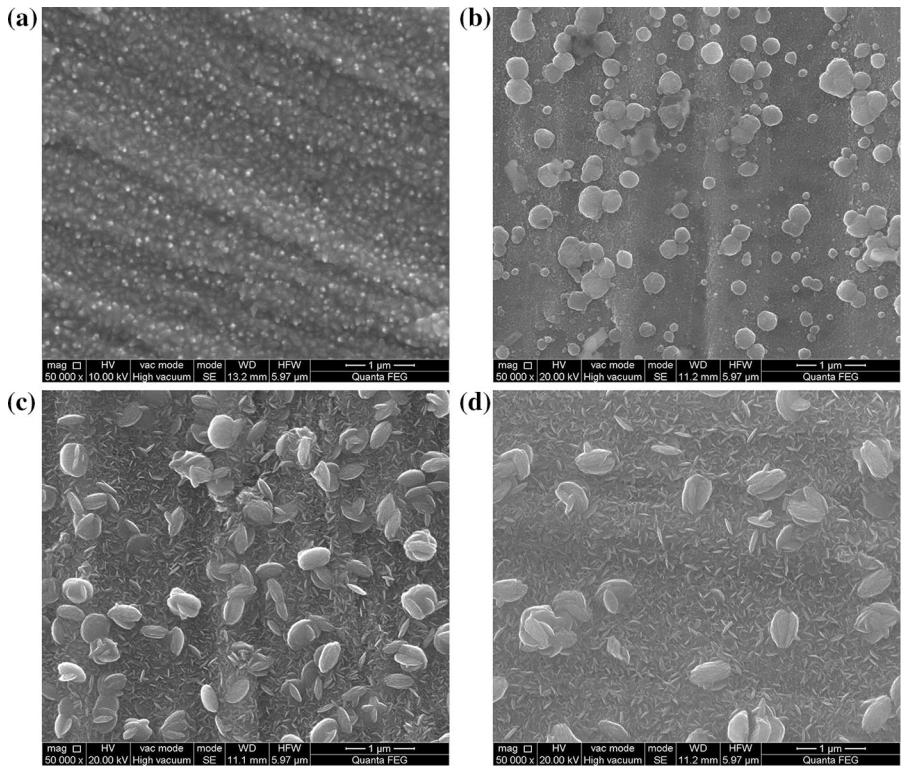

Fig. 1 SEM micrographs of the TLM samples: **a** S0, **b** S1, **c** S2, **d** S3

the two peaks located at 209.8 eV ($3d_{3/2}$) and 207.0 eV ($3d_{5/2}$) indicate that the bonding of Nb is in the form of Nb_2O_5. The Ca 2*p* peaks (350.7, 347.2 eV) and P 2*p* peak (133.2 eV) confirm calcium phosphate formed at the sample surface (Chusuei et al. 1999). In O 1*s* spectrum, the sub-peak P1 located at 530.0 eV can be assigned to TiO_2 and Nb_2O_5 (Fu et al. 2011b; Chen et al. 2011). The sub-peak P2 at 531.0 eV accompanied by the P 2*p* peak at 133.2 eV is diagnostic of hydroxyapatite, rather than $CaHPO_4{\cdot}2H_2O$ (Chusuei et al. 1999). The sub-peak P3 positioned at even higher bonding energy (532.2 eV) is attributed to hydroxyl groups at the sample surface.

Crystallography analysis

Hydrothermal method is widely employed to synthesize TiO_2 and alkaline-earth titanate with high purity, and the mechanism of the reactions has been established as a dissolution–precipitation process (Shi et al. 2012). XRD patterns of the hydrothermally treated TLM alloy samples are shown in Fig. 4. Apart from the diffraction peaks of the alloy substrate, only anatase peaks are present for the samples treated in calcium phosphate solutions. Although Nb_2O_5 is detected by XPS, the diffraction peaks of monoclinic Nb_2O_5 are absent, which has various standard

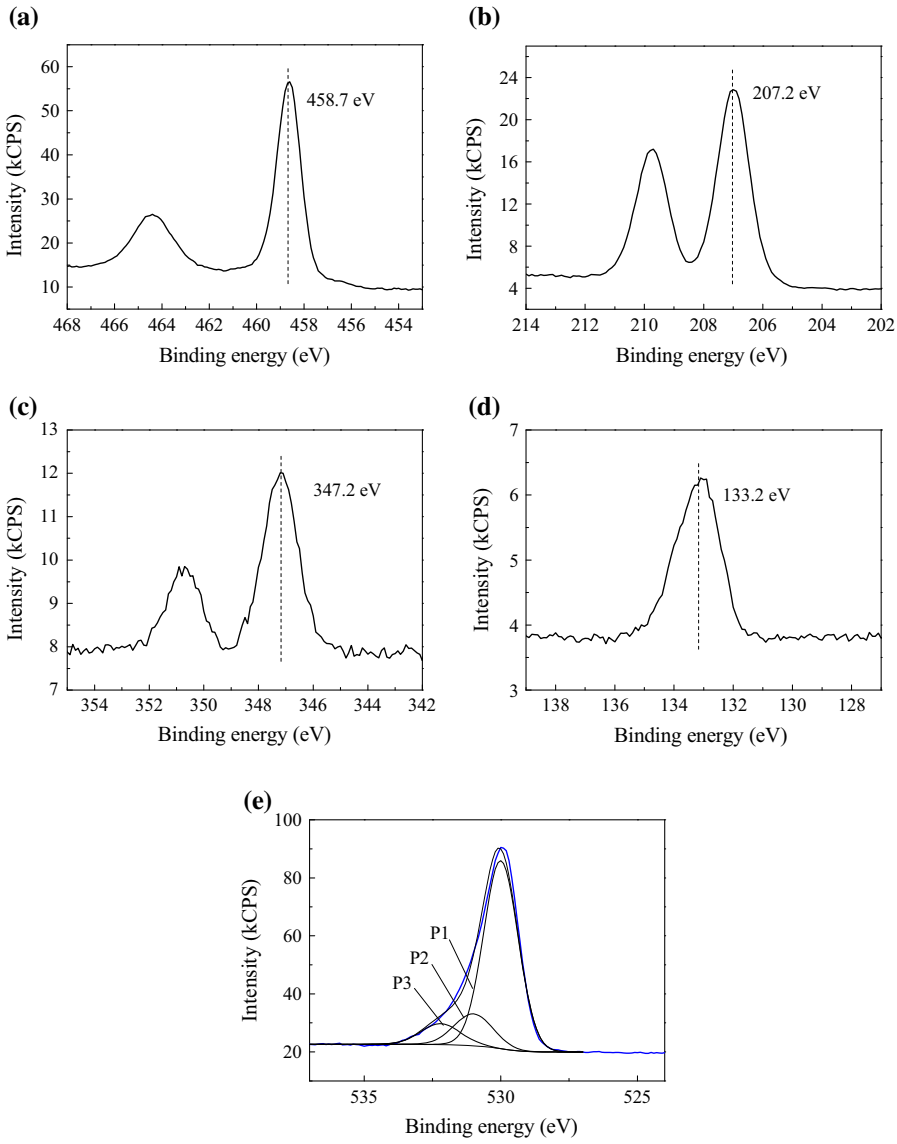

Fig. 3 XPS spectra of the TLM sample S2: **a** Ti 2*p*, **b** Nb 3*d*, **c** Ca 2*p*, **d** P 2*p*, **e** O 1*s*

diffraction patterns (ICDD #37-1468, #27-1311, #20-0804, etc.). Diffraction peaks of calcium phosphate are also absent, possibly due to the small film thickness. When $CaHPO_4{\cdot}2H_2O$ powder was hydrothermally treated at 200 °C for 16 h, diffraction peaks of hydroxyapatite were detected. This would suggest that the big particles shown in Fig. 1b–d are hydroxyapatite crystallites.

Bioactivity test

Bioactivity of TLM sample S2 was examined by the SBF test. After soaking for 6 days, the sample surface is covered by nano-fibrous deposits (Fig. 5a), and the nano-particles in Fig. 1c are not observed. In EDX spectrum, the peaks of Ca, P, and C are obviously increased, while the peaks of substrate elements are reduced (Fig. 5b), and the atomic ratio of Ca/Ti is increased from 0.38 before soaking to 8.51 after soaking. This reveals the formation of apatite layer containing carbonate ions. The tested side of the sample was faced downward during the soaking test, and so the deposit layer was formed by just adsorbing Ca^{2+}, PO_4^{3-}, CO_3^{2-}, and other ions from the solution. After soaking for 15 days, the peaks at $2\theta = 32.0°$ and 26.0° ascribed to apatite are present in the XRD pattern (Fig. 4d).

In the SBF test, the hydrothermally synthesized hydroxyapatite nano-crystallites may act as the nucleating sites for calcium phosphate growth. In addition, the negatively charged TiO_2 nano-grains due to the existence of hydroxyl groups (Fig. 3e) may favor the adsorption of Ca^{2+} ions to the film surface at the initial soaking stage (Viitala et al. 2002). The apatite layer then grows thick in SBF. The result demonstrates the in vitro bioactivity of the hydrothermally calcified TLM alloy.

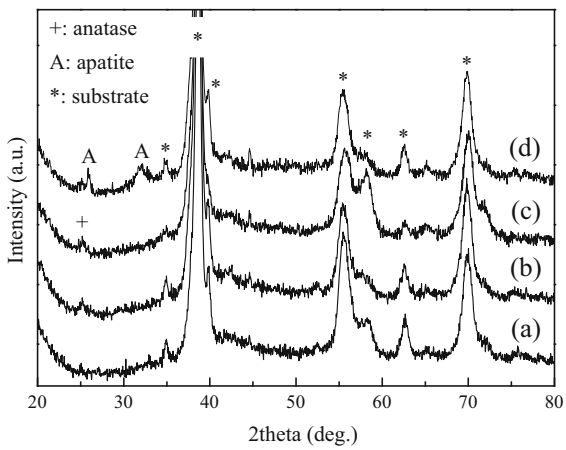

Fig. 4 XRD patterns of the TLM samples: **a** S1, **b** S2, **c** S3, **d** S2 soaked in SBF for 15 days

Corrosion test

Corrosion resistance of the TLM and Ti samples was tested by potentiodynamic polarization in 0.9 % NaCl solution (Fig. 6). The polished TLM sample has larger corrosion current density (I_{corr}), but higher corrosion potential (E_{corr}) than the hydrothermally treated sample S2. For the polished sample, a relatively stable passive current density ($I_{pass} = 3.455$ μA/cm^2) and a high pitting potential ($E_{pit} = 1.33$ V) are obtained after a long range of anodic polarization (Table 2). During

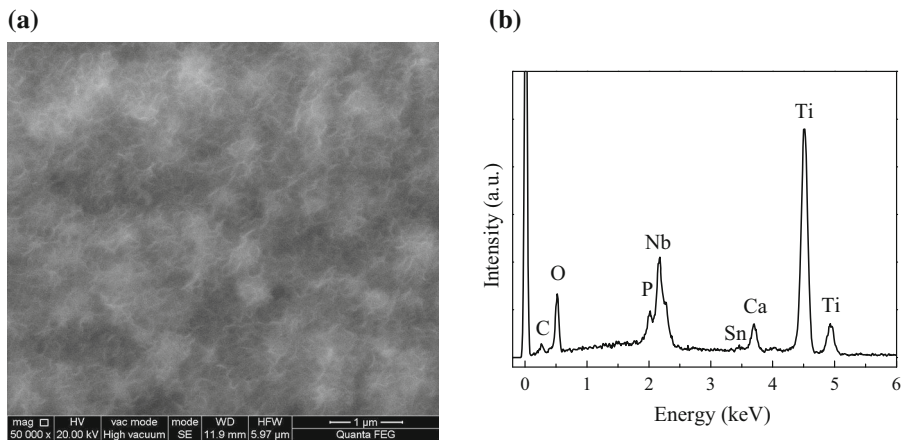

Fig. 5 **a** SEM micrograph and **b** EDX spectrum of the TLM sample S2 soaked in SBF for 6 days

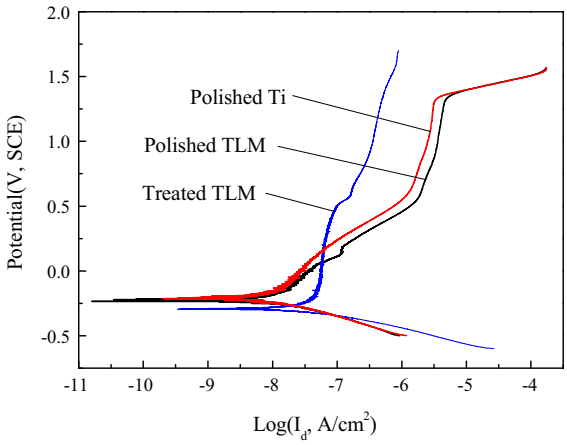

Fig. 6 Potentiodynamic polarization curves of **a** the polished TLM sample and **b** the hydrothermally treated sample S2 tested in 0.9 % NaCl solution

Table 2 Corrosion test data of the Ti and TLM samples

Sample	I_{corr} (nA/cm^2)	E_{corr} (V SCE)	E_{pit} (V SCE)	E_{pass} (V)	I_{pass} (μA/cm^2)
Polished Ti	2.51	−0.23	1.32	0.50	2.349[a]
Polished TLM	7.75	−0.22	1.33	0.76	3.455[a]
S2	7.35	−0.29	>1.70	>1.87	0.236[a]

[a] Value at the middle potential of the passivation region, E_{pass}

the anodic polarization, the dissolution of alloy elements leads to the increased anodic current density in comparison with that of the polished Ti sample (Fig. 6), and the current density becomes relatively stable when a resistant titania film is finally formed at the sample surface. Sample S2 has a higher pitting potential, a longer passivation region (E_{pass}) and a much lower passive current density ($I_{pass,}$ ~1/15) than the polished sample. The hydrothermally grown hydroxyapatite-TiO_2 (Nb_2O_5) film has effectively improved corrosion resistance of TLM alloy, which would be good for its biological properties.

Conclusion

The TLM alloy was hydrothermally treated in concentrated calcium phosphate solutions. The treated surface layers are composed of hydroxyapatite crystallites (100–500 nm) and small TiO_2 nanograins. Ti and Nb present as TiO_2 and Nb_2O_5 at the surface. The calcified TLM alloy exhibits bioactivity in SBF test and it has high corrosion resistance. The present work would provide a good method suitable for bioactive surface modification of Ti–Nb-based alloy implants with complex shapes and even pores (e.g., implants for cancellous bone and osteoporosis repairment).

Acknowledgments This work was financially supported by the Science and Technology Program of Shaanxi Province (No. 2015JM5152), the National Natural Science Foundation of China (No. 51202015), and the Fundamental Research Fund for the Central Universities (No. xjj2015072).

References

Chen XB, Li YC, Du Plessis J, Hodgson PD, Wen C (2009) Influence of calcium ion deposition on apatite-inducing ability of porous titanium for biomedical applications. Acta Biomater 5:1808–1820

Chen L, Sun QQ, Gu JJ, Xu Y, Ding SJ, Zhang DW (2011) Bipolar resistive switching characteristics of atomic layer deposited Nb_2O_5 thin films for nonvolatile memory application. Curr Appl Phys 11:849–852

Chusuei CC, Goodman DW, Van Stipdonk MJ, Justes DR, Schweikert EA (1999) Calcium phosphate phase identification using XPS and time-of-flight cluster SIMS. Anal Chem 71:149–153

Fu T, Wang C, Guo Z (2011a) Alkali treatment and bioactivity of medical near & #x03B2;-type titanium alloy TLM. Rare Metal Mater Eng 40:889–891

Fu T, Liu BG, Zhou YM, Wu XM (2011b) Sol-gel titania coating on NiTi alloy with a porous titania film as interlayer. J Sol-Gel Sci Technol 58:307–311

Fu T, Li HW, Sun JM, Li G, Li W, Zhang HM (2015) Facile hydrothermal synthesis of TiO_2-CaP nano-films on Ti6Al4V alloy. Trans Nonferrous Metals Soc China 25:1122–1127

Hamada K, Kon M, Hanawa T, Yokoyama K, Miyamoto Y, Asaoka K (2002) Hydrothermal modification of titanium surface in calcium solutions. Biomaterials 23:2265–2272

Kim HM, Miyaji F, Kokubo T, Nakamura T (1997) Effect of heat treatment on apatite-forming ability of Ti metal induced by alkali treatment. J Mater Sci-Mater Med 8:341–347

Lin JG, Li YC, Wong CS, Hodgson PD, Wen CE (2009) Degradation of the strength of porous titanium after alkali and heat treatment. J Alloy Compd 485:316–319

Nakagawa M, Zhang L, Udoh K, Matsuya S, Ishikawa K (2005) Effects of hydrothermal treatment with $CaCl_2$ solution on surface property and cell response of titanium implants. J Mater Sci-Mater Med 16:985–991

Qu J, Lu X, Li D, Ding YH, Leng Y, Weng J, Qu SX, Feng B, Watari F (2011) Silver/hydroxyapatite composite coatings

on porous titanium surfaces by sol-gel method. J Biomed Mater Res Part B 97B:40–48

Ryan G, Pandit A, Apatsidis DP (2006) Fabrication methods of porous metals for use in orthopaedic applications. Biomaterials 27:2651–2670

Shi XL, Nakagawa M, Kawachi G, Xu LL, Ishikawa K (2012) Surface modification of titanium by hydrothermal treatment in Mg-containing solution and early osteoblast responses. J Mater Sci-Mater Med 23:1281–1290

Viitala R, Jokinen M, Peltola T, Gunnelius K, Rosenholm JB (2002) Surface properties of in vitro bioactive and non-bioactive sol-gel derived materials. Biomaterials 23:3073–3086

Xiong JY, Li YC, Wang XJ, Hodgson P, Wen C (2008) Mechanical properties and bioactive surface modification via alkali-heat treatment of a porous Ti-18Nb-4Sn alloy for biomedical applications. Acta Biomater 4:1963–1968

Yamaguchi S, Kizuki T, Takadama H, Matsushita T, Nakamura T, Kokubo T (2012) Formation of a bioactive calcium titanate layer on gum metal by chemical treatment. J Mater Sci-Mater Med 23:873–883

Yu Z, Zhou L (2006) Influence of martensitic transformation on mechanical compatibility of biomedical & #x03B2; type titanium alloy TLM. Mater Sci Eng A 438:391–394

Zhang QY, Leng Y, Xin RL (2005) A comparative study of electrochemical deposition and biomimetic deposition of calcium phosphate on porous titanium. Biomaterials 26:2857–2865

Zheng CY, Li SJ, Tao XJ, Hao YL, Yang R, Zhang L (2007) Calcium phosphate coating of Ti-Nb-Zr-Sn titanium alloy. Mater Sci Eng C 27:824–831

Zheng CY, Li SJ, Tao XJ, Hao YL, Yang R (2009) Surface modification of Ti-Nb-Zr-Sn alloy by thermal and hydrothermal treatments. Mater Sci Eng C 29:1245–1251

Zhou Y, Wang YB, Zhang EW, Cheng Y, Xiong XL, Zheng YF, Wei SC (2009) Alkali-heat treatment of a low modulus biomedical Ti-27Nb alloy. Biomed Mater 4:044108